



## Controlled Ag Electroless Deposition in Bulk Structures with Complex Three-Dimensional Profiles

Radu Malureanu,<sup>2</sup> Maksim Zalkovskij,  
Andrei Andryieuski, and Andrei V. Lavrinenko

*Metamaterials Group, Fotonik Department, Technical University of Denmark, DK-2800, Kongens Lyngby, Denmark*

In this work we show the possibility of controlled deposition of a nanometer-sized silver layer on three-dimensional (3D) structures. The deposition takes place in liquid environment, allowing for an easy and fast processing with intrinsically isotropic characteristics. The obtained layers are of high uniformity, having an average roughness of about 4 nm. The characterization of the metal deposition is done using both the scanning electron microscopy technique as well as by atomic force microscope measurements. The electroless technique can be easily implemented, providing the effective and reliable metal deposition for fabrication of 3D samples in the broad range of plasmonics and photonics applications.

© 2010 The Electrochemical Society. [DOI: 10.1149/1.3502640] All rights reserved.

Manuscript submitted July 30, 2010; revised manuscript received September 21, 2010. Published October 21, 2010.

Deposition of thin, smooth metal layers on three-dimensional (3D) structures is one of the challenges within the thin film deposition field. Such structures have been proved to be extremely useful in a number of research fields and applications ranging from the Raman spectroscopy to metamaterials, from electronics to medicine. More specifically, correctly conceived metal covered surfaces can enhance the Raman spectra with several orders of magnitude.<sup>1</sup> Using deposition of metals from solution, one can obtain new ways for connecting the various components of electronic circuits.<sup>2,3</sup> The miniaturization of such circuits leads to increased requirements in the control of the deposition characteristics. Metal covered spherical particles have huge potential for several applications.<sup>4</sup> In the nanooptics, 3D metal-dielectric composites are the principal structural parts in new materials exhibiting extraordinary optical properties.<sup>5-9</sup> Such materials are called metamaterials since they have functionality beyond the known natural ones. In this work we concentrate on isotropic metal deposition on 3D samples with complex topology, which are aimed for metamaterials research. However, the applicability of such technique has emerging potential for much broader area than the presented example.

In the field of metamaterials, one direction is to extend the designs to truly 3D ones that can give bulk and eventually isotropic optical response within the frequency range of interest. A layer by layer approach for fabrication of 3D metamaterials in the infrared region has been demonstrated.<sup>10,11</sup> This fabrication process involving planarization, lateral alignment, and stacking is complicated and can provide only limited thickness of the resulting 3D metamaterial due to accumulation of unavoidable misalignments.

An alternative approach is the fabrication of a 3D polymer skeleton structure with further partial or complete metallization of its surface. The two-photon polymerization technique (2PP)<sup>12</sup> is proven to be very flexible and efficient technology for fabrication of 3D polymer layouts, including structures for photonic applications. Its potential in photonics has been confirmed by successful fabrication of woodpile constructions considered as efficient 3D photonic crystals with pronounced photonic bandgaps.<sup>13-16</sup> Still, even if various designs of 3D metamaterials have been proposed,<sup>17-20</sup> their manufacturability is hampered by the difficulty of the controlled metal deposition on 3D structures with complex topology.

To the best of our knowledge, there are two main methods for depositing metals on a 3D dielectric structure. The first one is based on the chemical vapor deposition (CVD), and the second is the electroless deposition technique. The CVD method shows great promise for depositing metals on the desired three-dimensional structure;<sup>21</sup> however, the parameter space for such technique is large; thus, the optimizing procedure claims exhaustive efforts due

to the existence of multiple local minima. The electroless deposition technique provides much more reduced parameter space, thus easier optimization, and lack of volatile poisonous products in the deposition process.

The electroless technique is based on the existence of a metallic complex dissolved into a solution and then its reduction to the constituent metal at structure's surface.<sup>22</sup> Some features are generated by the liquid environment that this technique needs, thus making it both cheaper for utilization and less sensitive to dust particles. The equipment used can be found in virtually any chemical laboratory, making its implementation extremely easy and cheap. Another important advantage of the electroless deposition is that the method is intrinsically isotropic; therefore, it offers the possibility of metal deposition on 3D structures irrespective of its shape and topology. Also, using such technique one can, by selectively treating the sample, control where the deposition takes place. Hence, in principle, silver can be deposited only at prescribed locations.<sup>23</sup> Unlike the conventional metal deposition techniques that are limited to low aspect-ratio structures (evaporation, sputtering) or need a conductive substrate (electrochemical growth), the electroless method can be used for depositing metal on almost arbitrary aspect-ratio patterns and substrates. This characteristic allows the use of such method to cover and fill in topologically complex 3D patterns and profiles and also create high-aspect-ratio metallized structures on dielectric substrates.

Following the list of these arguments, we decided to put our efforts in developing a solution-based method (electroless) for isotropic deposition of silver layers. Silver was chosen due to preferences in material parameters, in particular, the high plasma and low collision frequencies. There are different recipes for making the electroless deposition of silver, each having its own pros and cons. To our knowledge, the best result in silver depositing for metallization of photonic structures has been shown so far by Chen et al.<sup>24</sup> For this purpose, they used the three-step recipe. The initial step consists in binding of alkyl-amine groups to the surface of interest, followed by binding of gold nanoparticles to aminated sites. The final step is the silver deposition. The presented recipe shows selectivity between the substrate and the polymer structures, but, in the same time, the grain sizes were big, leading to increased roughness and layer thickness. As a result the reported layers were about 200–300 nm thick.<sup>24</sup> The recipe is a nice example of possibilities the electroless deposition technique presents, but it needs more refinement in order to reach the smoothness and thickness control required for the optical metamaterial structures. One of the best silver electroless plating results were published by Koo et al.<sup>25</sup> The Ag layers are both thin and very smooth, but unfortunately the TiN substrate cannot be used for photonic applications due to very high losses in the optical domain. In our paper we propose an alternative method that uses pretreatment with SnCl<sub>2</sub>. The experimental method and

<sup>2</sup> E-mail: rmal@fotonik.dtu.dk

chemical recipes are presented in the Experimental section and the quality of deposited silver layer is shown and discussed in the section Results and Discussion.

### Experimental

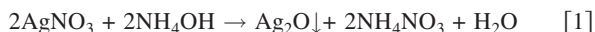
**Preparation of silica surface.**—The silica surface used for the first proof-of-principle and following optimization of the deposition characteristics was obtained by plasma enhanced chemical vapor deposition (PECVD) in an surface technology systems (STS) equipment. Deposition was performed in  $\text{SiH}_4/\text{N}_2\text{O}/\text{N}_2$  atmosphere. The power and pressure used were 60 W and 550 mTorr, respectively. Using the 12, 1420, and 392 sccm flows for  $\text{SiH}_4$ ,  $\text{N}_2\text{O}$ , and  $\text{N}_2$ , we obtain a deposition rate of  $81 \text{ nm min}^{-1}$  with better than 1% uniformity. The total deposition time was 15 min, thus depositing  $\sim 1.2 \text{ }\mu\text{m}$  of silica.

**Preparation of 3D samples.**—The samples were fabricated by 2PP on IP-L resist using the Nanoscribe system.<sup>26,27</sup> The photoresist layer was deposited on a 1-in., 150- $\mu\text{m}$ -thick glass slide. The laser beam was focused into the volume of the photoresist through the glass slide by the oil immersion 100 $\times$  microscope objective with numerical aperture 1.4.

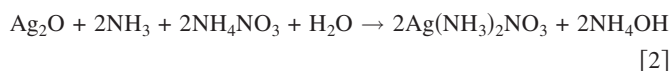
**Surface treatment for adhesion improvement.**—In order to improve the adhesion of a Ag layer on silica and IP-L surfaces, the sample was immersed in acidic solution of  $\text{SnCl}_2$ .<sup>28</sup> The total immersion time was 10 min and then the samples were thoroughly rinsed in distilled running water for 15 min. One shall not underestimate importance of rinsing the samples, since the silver deposit solution is readily contaminated, and thus the reducing process is not optimal.<sup>28</sup> Once the samples are surface treated, the silver deposition takes place.

**Silver layer deposition.**—We decided to obtain thin and smooth metallic layers by optimizing the recipe known as Tollen's test or the silver mirror reaction.<sup>28</sup> Within such recipe the three main reaction steps are as follows:

1. Diluted solution of silver nitrate reacts with ammonia hydroxide in order to form brown precipitate (silver oxide)



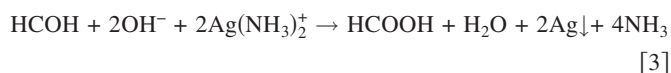
2. By careful continuous adding of ammonia hydroxide, the solution becomes transparent again, thus showing the formation of ammoniacal silver nitrate



which further readily splits into its polar constituents



3. At this point the silver compound is fully formed and can be reduced to silver and ammonia. The reducing reaction takes place in the presence of aldehyde (formaldehyde in our case) and is generally used for determining the presence of such aldehydic groups



Even if the reaction process is well understood, the practical implementation is not a direct one. The first challenge is the instability of the ammoniacal silver nitrate solution; thus, it was prepared every time from stock solutions. The first solution is obtained by mixing 2.5 mL 0.2 mol  $\text{AgNO}_3$  with 0.114 mL 25%  $\text{NH}_3$ . At the beginning,  $\text{Ag}_2\text{O}$  is formed in the phase of brown precipitate. Ammonia hydroxide is added continuously to carry on the reaction until the silver ammonia complex is obtained. The solution is then diluted in MilliQ water in order to obtain 5 mL of reagent. The second solution is the 8% formaldehyde solution. The deposition procedure involves immersing the surface treated sample in 30 mL MilliQ wa-

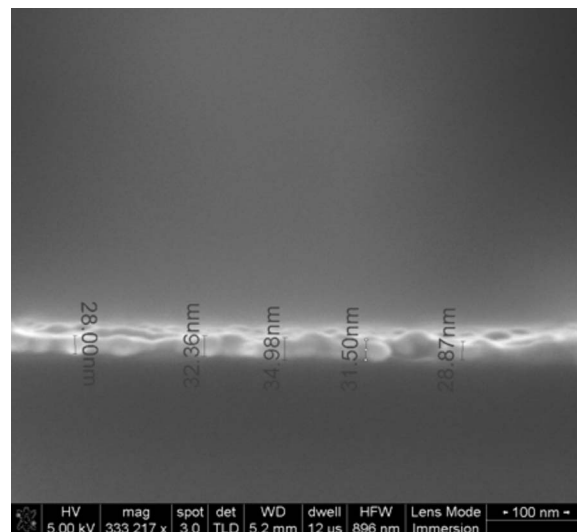


**Figure 1.** Ultrathin uniform silver layer deposited by the electroless technique on the silica substrate. Numbers show the thickness of the silver coating.

ter and then adding 500  $\mu\text{l}$  of diluted formaldehyde and the silver ammonia complex solutions. The solution becomes dark and the reaction takes place. At room temperature, due to the fast reaction time, the reaction is difficult to control; therefore, the solutions are cooled down to  $5^\circ\text{C}$ . The deposited silver film thickness varies with the immersion time, having the approximate growth rate of  $30 \text{ nm min}^{-1}$  at this temperature. After the layer has been formed, the samples are thoroughly rinsed in running water for 5 min.

The unreacted solution must be carefully disposed of and the containers used in the experiment must be thoroughly rinsed in order to prevent the formation of explosive silver nitride.

### Results and Discussion

Optimization steps in the above mentioned technique were made within the first rounds of tests on simple planar samples. The thinnest uniform silver layer obtained was of about 30 nm (Fig. 1). The layer thickness is directly proportional to the immersion time. Using the presented recipe, thicknesses of up to 200 nm have been achieved (not shown) simply by increasing the immersion time. Silver layers thinner than 30 nm are not completely formed, exhibiting random clusters formation. We think that this effect is due to the mechanism of the silver seeds growth in the solution. It can be inhibited, making possible deposition of thinner silver layers. In Fig. 2 we present a top-view showing high uniformity in the layer formation. The substrate is uniformly covered, but few silver nanoparticles can be observed on the top of its surface. These Ag nanocrystals are formed in the solution and then deposited in the ready form on sample's surface. Still, such nanocrystals' formation is minimal and does not restrain the overall deposition process. In the inset of Fig. 2, one can see a top-view of the layer at a higher magnification; thus, the polycrystalline growth of silver is noticeable. Our samples are up to  $1 \text{ cm} \times 1 \text{ cm}$  in sizes, and no pronounced difference in layer properties is noticeable over such extended surface. So it validates that such technique has no limitations by the depositing area and can be applied to samples of, in principle, whatever dimensions.

For optimizing the deposition technique, we employed the quantitative criteria of the average roughness calculated on a sample portion, where there are no Ag nanocrystals. The roughness was calculated from atomic force microscope (AFM) measurements obtained in the tapping mode. While single nanocrystals can reach dimensions of up to 100 nm, the average roughness in the "clean" areas is of the order of 4 nm and the roughness mean square value (rms) is about 6 nm, which is comparable with the rms for evapo-

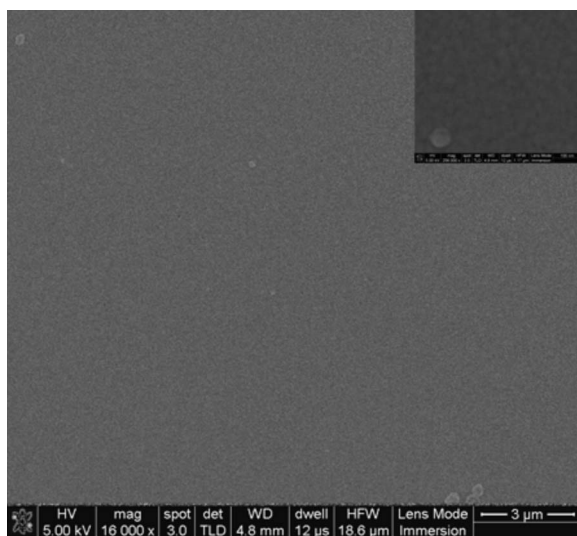


**Figure 2.** Top view of  $30 \times 30 \mu\text{m}$  sample's area showing high deposition uniformity over a large area (up to  $1000 \times 1000 \mu\text{m}$ ). Some single Ag nanocrystals deposited on top of the layer are visible. In the inset, a zoom-in of the surface is shown.

rated films (see Fig. 3). Taking into account that the substrate average roughness measured in the same conditions is 2 nm, we conclude that the metallic layer is adding approximately 2 nm in terms of rugosity.

Following the process optimized for flat surface we deposited a silver layer on a structure with 3D topology. As a sample for thorough checking of deposition on volumetric structures with complex profiles, we chose a 2PP polymer woodpile.<sup>29</sup> This way we were able to check the Ag deposition both on structure's sidewalls as well as in the bulk volume deep inside it. The woodpiles are  $100 \mu\text{m} \times 100 \mu\text{m}$  and have a height of about  $2 \mu\text{m}$  corresponding to two periods (eight single layers) of the lattice. Sizes of the bar cross-section are  $150 \text{ nm} \times 150 \text{ nm}$ . Such woodpiles possess a face centered tetragonal lattice. We immersed them into the deposition bath for 2 min. This produces approximately 50-nm-thick regular silver covering of the woodpile surfaces. Results of the silver deposition are presented in Fig. 4. The Ag layer is deposited not only on the top of the structure but also on its sidewalls. There is still particle formation in the solution followed by their adhesion to the deposited layer, but it can be further minimized. Upon inspecting the metallized structure at higher magnification (Fig. 5) we can observe the

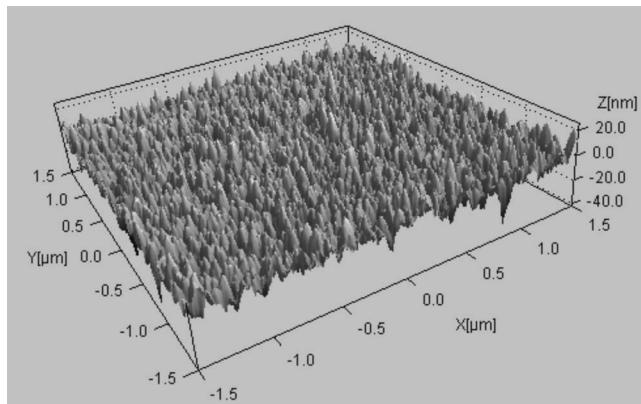


**Figure 3.** 3D AFM image used for roughness analysis. The average roughness of 4 nm with an rms of 6 nm was calculated excluding the areas with silver clusters on.

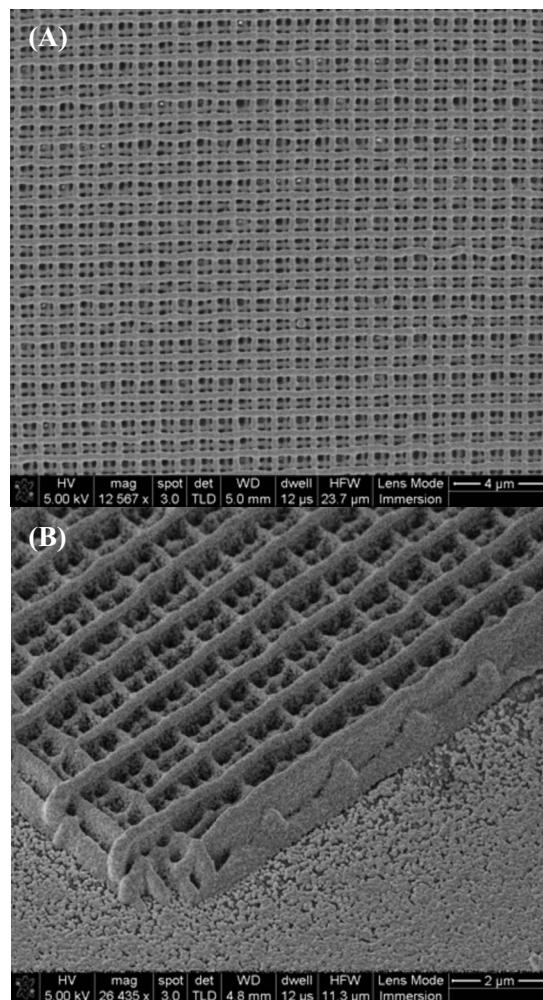


**Figure 4.** A 3D woodpile structure covered by silver after electroless deposition. (A) Top view of the sample showing uniform deposition over a big surface area. (B) Tilted imaging showing deposition on the structure's sidewalls.

presence of the silver layer inside the bulk structure as well. The layer quality when depositing on a 3D structure is different from the one on a plane silica surface. We believe that this dissimilarity is mainly due to the modified surface chemistry of IP-L polymer used in the 2PP fabrication of the 3D samples.

One should note that the reaction is diffusion driven. Due to this aspect, the silver layer quality is monotonously degrading from the top to the bottom of the structure (Fig. 6). Nevertheless, deposition took place everywhere, covering the whole woodpile with a 50-nm-thick silver layer in one 2-min approach only. With further optimization and decreasing of the reaction speed, the degradation of coating in depth can be minimized.

The surface pretreatment is an important part of the process. To prove its significance we tried to deposit silver without pretreatment. As it can be seen from Fig. 7, in its absence, the silver layer is not adhering to the silica substrate. In the same time this nonadhesion shows that, if needed, silver can be selectively deposited on a structure by deliberate pretreatment of the surface.

The obtained results are easily reproduced on various samples of different dimensions as long as the deposition conditions are the same.

## Conclusions

One of the main bottlenecks in advancing the fabrication of metamaterials is due to the difficulty of realizing low-cost isotropic



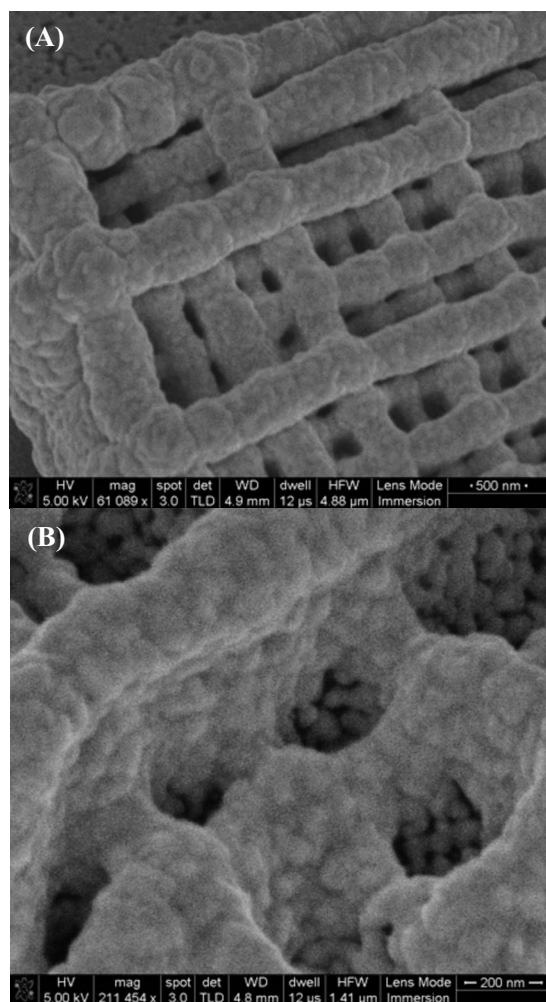


**Figure 5.** High magnification SEM image of the 3D structure showing the deposition took place also inside the woodpile. (A) 60 K magnification showing deposition of Ag several layers inside the woodpile. (B) 200 K magnification allowing the inspection of the Ag deposition inside small dimension holes.

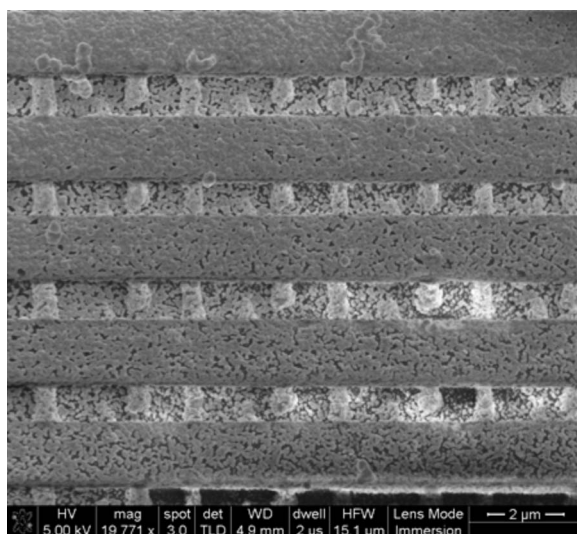


**Figure 6.** Sidewall SEM image of a 3D periodic structure made by 2 photon-polymerization. As can be seen, the deposited layer's quality decreases from the top to the bottom of the structure. Here five periods in the vertical direction are presented.

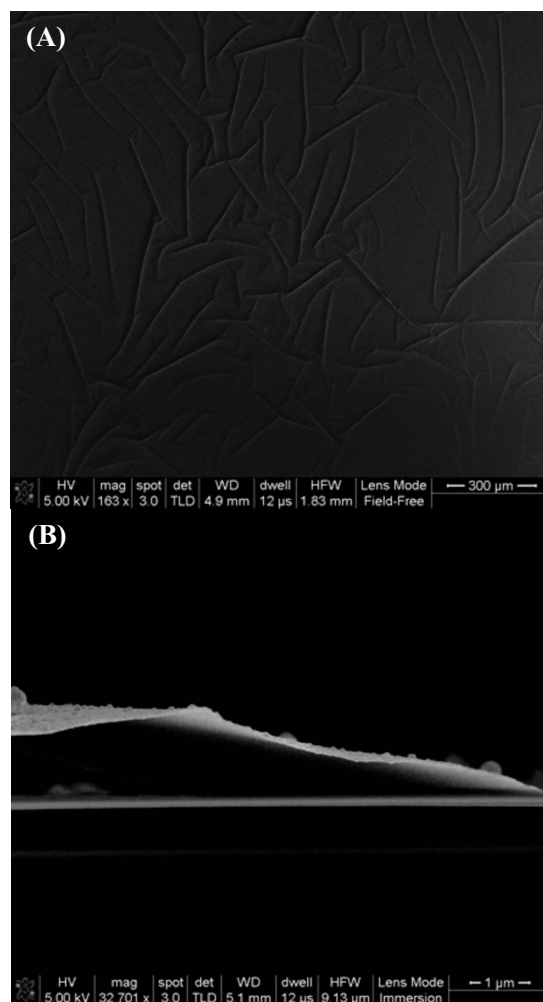


**Figure 7.** Example of weak adhesion of the silver layer to the untreated silica surface. It illustrates the importance of pre-treatment for good adhesion. (A) Top view of a layer with weak adhesion. (B) Cross-section showing the detachment of the Ag layer from the untreated silica surface.

3D deposition of metals on desired structures. We believe that by using a combination of the electroless deposition and 2PP techniques a viable solution for fabricating 3D bulk metamaterials can be found. In this work we present the optimized method for depositing silver on silica and IP-L polymer.

Such technique is not limited to the metamaterials field, but it can be used in other research areas where depositing of metals are required. For example, depositing metal on rough surfaces can be a way of improving the Raman signal in surface enhanced Raman spectroscopy up to several orders of magnitude.<sup>1</sup> Also, metal deposition proves itself useful in various industry-related applications ranging from electronics<sup>2</sup> up to medicine.<sup>4</sup> In the same time, the electroless technique may serve as a valuable tool for the photonics devices fabrication since one can accurately control the deposition characteristics. We think that the technique reported here bears great potential in many aspects of metal deposition in nanophysics and nanotechnology.

#### Acknowledgments

R. Malureanu, A. Andryieuski, and A. Lavrinenko acknowledge the partial financial support from the NIMbus project funded by the Danish Research Council for Technology and Production Science.

*Technical University of Denmark assisted in meeting the publication costs of this article.*

## References

1. A. Campion and P. Kambhampati, *Chem. Soc. Rev.*, **27**, 241 (1998).
2. C.-C. Cheng, V. M. Dubin, and P. K. Moon, U.S. Pat. 7,223,694 (2007).
3. T. Scheibel, R. Parthasarathy, G. Sawicki, X.-M. Lin, H. Jaeger, and S. L. Lindquist, *Proc. Natl. Acad. Sci. U.S.A.*, **100**, 4527 (2003).
4. S. Lal, S. E. Clare, and N. J. Halas, *Acc. Chem. Res.*, **41**, 1842 (2008).
5. V. Shalaev, *Science*, **322**, 384 (2008).
6. D. Schurig, J. J. Mock, B. J. Justice, S. A. Cummer, J. B. Pendry, A. F. Starr, and D. R. Smith, *Science*, **314**, 977 (2006).
7. A. Degiron, D. R. Smith, J. J. Mock, B. J. Justice, and J. Gollub, *Appl. Phys. A*, **87**, 321 (2007).
8. M. W. Klein, C. Enkrich, M. Wegener, and S. Linden, *Science*, **313**, 502 (2006).
9. N. I. Landy, S. Sajuyigbe, J. J. Mock, D. R. Smith, and W. J. Padilla, *Phys. Rev. Lett.*, **100**, 207402 (2008).
10. N. Liu, H. Guo, L. Fu, S. Kaiser, H. Schweizer, and H. Giessen, *Nature Mater.*, **7**, 31 (2008).
11. N. Liu, H. Liu, S. Zhu, and H. Giessen, *Nat. Photonics*, **3**, 157 (2009).
12. S. Maruo, O. Nakamura, and S. Kawata, *Opt. Lett.*, **22**, 132 (1997).
13. M. Deubel, G. von Freymann, M. Wegener, S. Pereira, K. Busch, and C. M. Soukoulis, *Nature Mater.*, **3**, 444 (2004).
14. J. Serbin, A. Ovsianikov, and B. Chichkov, *Opt. Express*, **12**, 5221 (2004).
15. N. Grossman, A. Ovsianikov, A. Petrov, M. Eich, and B. Chichkov, *Opt. Express*, **15**, 13236 (2007).
16. T. Ergin, N. Stenger, P. Brenner, J. B. Pendry, and M. Wegener, *Science*, **328**, 337 (2010).
17. I. Vendik, O. Vendik, and M. Odit, *Microwave Opt. Technol. Lett.*, **48**, 2553 (2006).
18. C. R. Simovski and S. A. Tretyakov, *Phys. Rev. B*, **79**, 045111 (2009).
19. A. Alù and N. Engheta, *Opt. Express*, **17**, 5723 (2009).
20. A. Andryieuski, R. Malureanu, and A. Lavrinenko, *J. Eur. Opt. Soc. Rapid Publ.*, **4**, 09003 (2009).
21. M. S. Rill, C. Plet, M. Thiel, I. Staude, G. Von Freymann, S. Linden, and M. Wegener, *Nature Mater.*, **7**, 543 (2008).
22. J. Zhang, P. Zhan, H. Liu, Z. Wang, and N. Ming, *Mater. Lett.*, **60**, 280 (2006).
23. F. Formanek, N. Takeyasu, T. Tanaka, K. Chiyoda, A. Ishikawa, and S. Kawata, *Appl. Phys. Lett.*, **88**, 083110 (2006).
24. Y.-S. Chen, A. Tal, and S. M. Kuebler, *Chem. Mater.*, **19**, 3858 (2007).
25. H.-C. Koo, S. Y. Kim, S. K. Cho, and J. J. Kim, *J. Electrochem. Soc.*, **155**, D558 (2008).
26. G. von Freymann, A. Ledermann, M. Thiel, I. Staude, S. Essig, K. Busch, and M. Wegener, *Adv. Funct. Mater.*, **29**, 2061 (2004).
27. S. Kawata, H.-B. Sun, T. Tanaka, and K. Takada, *Nature*, **412**, 697 (2001).
28. R. W. Furness, *The Practice of Plating on Plastics*, Chap. 8, Robert Draper Ltd./Teddington Press, Surrey, U.K. (1968).
29. S. Y. Lin, J. G. Fleming, D. L. Hetherington, B. K. Smith, R. Biswas, K. M. Ho, M. M. Sigalas, W. Zubrzycki, S. R. Kurtz, and J. Bur, *Nature*, **394**, 251 (1998).